Published in final edited form as:
Hear Res. 2010 May ; 263(1-2): 78–84. doi:10.1016/j.heares.2009.11.005.

Motion of the Tympanic Membrane after Cartilage Tympanoplasty Determined by Stroboscopic Holography

Antti A. Aarnisalo, MD, PhD[1,2], **Jeffrey T. Cheng, PhD**[1,2], **Michael E. Ravicz, MSc**[1], **Cosme Furlong, PhD**[1,2,3,4], **Saumil N. Merchant, MD**[1,2,4], and **John J. Rosowski, PhD**[1,2,4]

[1] Eaton-Peabody Laboratory, Massachusetts Eye and Ear Infirmary, Boston, MA

[2] Department of Otology and Laryngology, Harvard Medical School, Boston, MA

[3] Department of Mechanical Engineering, Worcester Polytechnic Institute, Worcester, MA

[4] Division of Health Sciences and Technology, Harvard University-Massachusetts Institute of Technology, Cambridge MA

Abstract

Stroboscopic holography was used to quantify dynamic deformations of the tympanic membrane (TM) of the entire surface of the TM before and after cartilage tympanoplasty of the posterior or posterior-superior part of the TM. Cartilage is widely used in tympanoplasties to provide mechanical stability for the TM.

Three human cadaveric temporal bones were used. A 6 mm × 3 mm oval cartilage graft was placed through the widely opened facial recess onto the medial surface of the posterior or posterior-superior part of the TM. The graft was either in contact with the bony tympanic rim and manubrium or not. Graft thickness was either 0.5 or 1.0 mm. Stroboscopic holography produced displacement amplitude and phase maps of the TM surface in response to stimulus sound. Sound stimuli were 0.5, 1, 4 and 7 (or 8) kHz tones. Middle ear impedance was measured from the motion of the entire TM.

Cartilage placement generally produced reductions in the motion of the TM apposed to the cartilage, especially at 4 kHz and 7 or 8 kHz. Some parts of the TM showed altered motion compared to the control in all three cases. In general, middle ear impedance was either unchanged or increased somewhat after cartilage reconstruction both at low (0.5 and 1 kHz) and high (4 and 7 kHz) frequencies. At 4 kHz, with the 1.0 mm thick graft that was in contact with the bony tympanic rim, the impedance slightly decreased.

While our earlier work with time-averaged holography allowed us to observe differences in the pattern of TM motion caused by application of cartilage to the TM, stroboscopic holography is more sensitive to TM motions and allowed us to quantify the magnitude and phase of motion of each point on the TM surface. Nonetheless, our results are similar to those of our earlier work: The placement of cartilage on the medial surface of TM reduces the motion of the TM that apposes the cartilage. These obvious local changes occur even though the cartilage had little effect on the sound-induced motion of the stapes.

Corresponding author and address for reprints: Antti A. Aarnisalo, Dept. of Otorhinolaryngology, Helsinki University Central Hospital, POB 220, 00029 HUS Helsinki, Finland. Tel: +358 9 4711, Fax: +358 9 47175010, antti.aarnisalo@helsinki.fi; antti.aarnisalo@hus.fi.

Keywords

tympanic membrane; tympanoplasty; stroboscopic holography

INTRODUCTION

Cartilage is widely used in tympanoplasties to provide mechanical stability for the tympanic membrane (TM) (Yung, 2008; Tos, 2008), yet the effects of cartilage TM grafts on middle ear sound transmission have not been characterized in a systematic manner. Only a few studies have investigated the acoustics of cartilage TM grafts. Lee et al. (2006, 2007) used a finite element model analysis to study such grafting techniques and, suggested that a cartilage graft should be as thin as possible. Zahnert et al. (2000) and Murbe et al. (2002) studied the acoustic properties of cartilage grafts in an experimental setting. They measured the sound-induced motion of cartilage grafts placed at the end of an artificial ear canal without being loaded by the ossicles or cochlea, and concluded that in order for cartilage grafts to mimic the material properties of the TM the graft must be of thickness of 1.0 mm or less.

In the present study, we investigated the changes in motion of the TM after cartilage tympanoplasty using cadaveric temporal bone preparations with a novel technique: computer-assisted high-speed Opto-Electronic Holography (OEH) (Furlong et al. 2009; Rosowski et al. 2009; Cheng et al., 2009). OEH can be used to study the vibration of the whole TM (Rosowski et al, 2009). The main features of OEH are that the holographic interference patterns are digitized and the computation of the holographic images is enabled by the use of computer-controlled variations in the length of the optical path (Furlong and Pryputniewicz, 1998; Rosowski et al., 2009). OEH can be used in two modes: time-averaged and stroboscopic modes.

In a companion study (Aarnisalo et al., 2009) we used time-averaged holography to qualitatively describe the effects of cartilage placed on the medial surface of the posterior-superior TM on the patterns of TM motion. This study suggested that the cartilage had significant local effects on the motion pattern of TM especially at frequencies above 4 kHz; however, those changes were not associated with significant changes in sound-induced stapes velocity. Neither the position of the cartilage graft (either with contact of the bony tympanic rim or not) or varied thicknesses of cartilage of 1.0 mm or less had significant effects on the sound-induced stapes velocity. Therefore, small cartilage grafts of 1.0 mm thickness or less in the posterior-superior TM quadrant do not greatly affect middle-ear function irrespective of contact with the bony annulus (Aarnisalo et al., 2009).

Time-averaged holography is insensitive to the phase of motion relative to the sound stimulus phase. Wada et al. (2002) used a sinusoidal phase modulation technique to detect both amplitude and phase of motion of guinea pig TM from stroboscopic speckle pattern interferometry. Decraemer et al. (1999) used high-density laser-Doppler vibrometry to estimate the amplitude and phase of motion along a single diameter of the cat TM and de La Rochefoucauld et al. (2009) used similar techniques to describe the motion of a line across the gerbil TM.

In this report, we describe results using stroboscopic holography to study sound-induced motion of the TM with stimuli from 0.5 kHz to 8 kHz (Furlong et al., 2009; Hernandez-Montes et al., 2009; Cheng et al., 2009). Our technique is similar to that of Wada et al. (2002); however, we measured sound-induced differences in the optical phases of the interfering beams that vary over multiple optical wavelengths (Furlong and Pryputniewicz, 1998; Furlong et al. 2009). With stroboscopic holography we can quantify both the amplitude and phase of the dynamic deformations of the TM over the full field of view. The results better quantify how the normal

and grafted TM responds to sound, and allow us to calculate the middle-ear input impedance, a measure of the mobility of the entire TM.

MATERIAL AND METHODS

All of the measurements reported in this manuscript were performed concurrently with previously reported measurements of stapes velocity and time-averaged holograms of the sound-induced motion of the TM surface (Aarnisalo et al., 2009). The methods in common to the two reports are summarized below. The methods specific to stroboscopic holography are described in detail in Cheng et al. (2009).

Human temporal bones

Three fresh human temporal bones and pieces of conchal cartilage were obtained from donors of 63–87 years of age. All donors had no evidence of otologic disease, and the specimens were removed within 24 hours after death. The temporal bones were removed from the cranium with a circular saw following the procedures described by Schuknecht (1968). This study was approved by the Institutional Review Board of the Massachusetts Eye and Ear infirmary.

The bony external auditory canal was drilled away to the level of the tympanic ring in order to expose the lateral surface of the TM. The facial recess was widely opened. The tendon of the stapedius muscle was severed to enable visualization of the posterior crus for the stapes-velocity measurements described in our previous manuscript (Aarnisalo et al., 2009; Chien et al., 2006). The middle ear cavity was left open to the atmosphere during the measurements. The TM and middle ear cavity were kept moist by frequent spraying of saline and regular immersion in saline.

The temporal bone was held in a clamp and oriented as in a seated patient. The speculum of the sound coupler was positioned as close as possible to the TM such that the object beam of the laser was perpendicular to the tympanic ring (Hernández-Montes et al., 2009). To increase the light reflected from the nearly-transparent TM, the TM surface was painted with a suspension of TiO_2 powder (Acros Organics, Geel, Belgium) in saline. The effects of this paint on TM mechanics appear to be small (Rosowski et al., 2009).

Cartilage grafts

Pieces of conchal cartilage were cut into 0.5 mm and 1.0 mm thick cartilage sheets using a commercially available cutting device (Kurz Company, Dusslingen, Germany). The sheets were then cut with a sharp knife into oval shaped (6 mm × 3 mm) plates (Fig. 1). Either the 0.5 mm or 1.0 mm thick oval plate of conchal cartilage was placed on the medial TM surface in the posterior or posterior-superior quadrant through the wide opening of the facial recess. The cartilage plate was positioned so that it was either not in contact with the bony tympanic rim and manubrium (Fig. 1A), or in contact with these two bony regions (Fig. 1B).

Computer-Assisted Opto-Electronic Laser Holography

Motion of the TM was evaluated with computer-assisted opto-electronic laser holography (OEH). The OEH system was operated in stroboscopic holography mode, which allows identification of both phase and magnitude of TM motion (Furlong et al. 2009; Hernandez-Montes et al., 2009).

The exposed TM was mounted orthogonal to the long axis of the sound-coupler and the collimated object-illumination beam of a laser was focused through the coupler onto the TM surface. The reflected object beam of the OEH system was focused in the interferometric head where it mixed with the reference beam, and the subsequent interferogram was captured by a

computer-controlled digital camera. The sound coupler was connected to a Tucker-Davis CF1 speaker (Tucker-Davis Technologies, Alachua, Florida). A calibrated Knowles EK-3103 hearing-aid microphone (Knowles Electronics, Itasca, Illinois) and probe tube measured sound pressure near the edge of the TM. The sound stimuli were continuous tones of either, 0.5, 1, 4, 7 or 8 kHz and levels of 70 to 130 dB SPL. Each holographic image required four $1/30^{th}$ of a second exposures of the digital camera, where the optical path length of the reference beam was regularly shifted by lengths of either 0, 0.25, 0.5 and 0.75 wavelengths before each exposure (Furlong and Pryputniewicz, 1998; Rosowski et al., 2009).

In stroboscopic holography an acousto-optical modulator strobes the laser so that the light illuminates the object and the camera only during a brief period (10% of the period of the frequency of the tonal stimulus) during each cycle of the stimulus tone. Each camera image then represents the summed response to a large number of strobe impulses. To describe the variations in TM displacement with the phase of the stimulus, a holographic image (each calculated from 4 camera exposures as described above) was gathered at each of eight stroboscopic phases of either 0°, 45°, 90° … 315° relative to the zero crossing of the sinusoidal stimulus driving the earphone.

Analysis of TM motion from stroboscopic holography images

Each of the eight strobe holograms describe the phase-locked sound-induced variation in the optical phase of the reflected object beam relative to the reference beam. These phase changes are related to the relative displacement of the TM between each strobe pulse but are wrapped in phase modulo $\pm \pi$. Spatial phase-unwrapping algorithms, developed at the Worcester Polytechnic Institute (Furlong and Pryputniewicz, 1998; Furlong et al., 2009), were used to describe displacement-induced changes in the optical path length that varied over multiple wave-lengths of the laser light. The differences in the unwrapped path length between subsequent stroboscopic images are scaled versions of the TM displacements that occurred between the strobe pulses. While generally robust, the unwrapping algorithm is sensitive to rapid variations in the optical phase that are sometimes seen at the edges of the TM, or at locations where the TiO_2 paint is not homogenous. Masks are used to exclude such transitions from further analysis (Furlong et al., 2009; Cheng et al., 2009).

Displacement amplitude and phase maps of the TM surface were produced with Matlab (Mathworks, Natick, Massachusetts) (Cheng et al., 2009). The measured displacements were normalized by the sound pressure level of each stimulus. We also investigated the magnitude and phase of TM motion along individual chords across the TM surface and, the most useful chord was positioned 45° relative to the horizontal that went through the umbo and the 90° diameter defined by the manubrium (Fig. 2). This chord went through the area of the TM that was covered by the cartilage sheets.

Impedance measurements

Once the magnitude and phase of displacement was known for each point on the surface of the TM, we estimated the volume velocity of the TM by summing the complex (magnitude and phase) displacement values and multiplying by the pixel area and by $\sqrt{-1}$ times the radian frequency of the sound ($2\pi \times$ sound frequency in Hz). The ratio of the measured sound pressure and the computed volume velocity is the middle-ear input impedance (Cheng et al., 2009). The results from the three bones for each condition were averaged and the different conditions were compared with the control measurement.

RESULTS

Displacement amplitude of the whole TM

Contour maps of the magnitude of motion on the surface of one TM in the different conditions are illustrated in Figure 3. The displacements are normalized by the stimulus sound pressure. At 0.5 kHz the site of the maximum displacement is in the posterior superior-quadrant in all cases and the maximal normalized displacement is similar across all condition. At 1 kHz, four of the 5 conditions (including the control) show the maximum in normalized displacement in the posterior-superior quadrant. The patterns of displacement also appear more variable. At 4 and 7 kHz the cartilage sheet produces a significant reduction in the motion of the TM apposed to the sheet regardless of the thickness or the orientation of the sheet. The cartilage also seems to produce smaller changes in displacement at other TM locations.

Displacement Amplitude along a Chord trough the position of the cartilage

Displacement magnitudes on the TM surface along a chord through the area of cartilage placement measured at 1 kHz and at 4 kHz in all three bones are illustrated in Figure 4. The data at 0.5 kHz (not shown) are similar to the results at 1 kHz frequencies, and the data at 7 or 8 kHz (not shown) are similar to the data at 4 kHz. At 1 kHz (Figure 4A) the control displacements along the chord show a clear peak near the 4 mm position, which maps to the posterior-superior quadrant of the TM. Placement of the cartilage sheet of either thickness or either orientation reduces the magnitude of motion in the region where the cartilage apposes the TM (the blue bar in the space domain). The cartilage has smaller effects on regions of the membrane where there is no contact. The thicker cartilage sheet tends to produce larger reductions in displacement. While we see the largest cartilage-induced reductions in motion in the areas that move the most, those are also the areas where we place the cartilage.

At 4 kHz, there are multiple peaks in displacement magnitude along the chord we have chosen. In the control condition, there tends to be a larger number of sharper displacement maxima in the anterior-inferior quadrant (positions −4 to 0). The placement of the cartilage sheet greatly reduces the motion of regions in contact with the cartilage in bones 11 and 12; the exception is the 1.0 mm thick graft with bone contact condition (BC) in TB11, where the reduction is less pronounced. In those same bones, the effect of the cartilage on positions not directly in contact with the cartilage is generally small. In TB 10 the cartilage effects are different. The 1 mm cartilage placement leads to an increase in motion magnitude in the region contacted by the cartilage, and we also see significant alterations in displacement magnitude at regions not in contact with the cartilage sheet.

Middle ear Impedance

We calculated the input impedance at the TM and compared our results to earlier results (Table 1). At 1 kHz, the impedance magnitudes we estimate are very similar to that measured by Rabinowitz (1981) and others using acoustic techniques. However, the impedances we calculate at 0.5 and 4 kHz are significantly larger than Rabinowitz's estimates, and the impedances at 7 and 8 kHz are even larger in magnitude. We also plot the change in middle-ear impedance magnitude relative to the control (Figure 5). Increases in impedance magnitude are associated with a decrease in the computed volume-velocity of the TM, while decreases in impedance are due to an increase in the computed volume-velocity. In general, the data suggest that the placement of cartilage in the posterior-superior quadrant produced 5 to 10 dB increases in the middle ear impedance at 0.5, 1 and 4 kHz; but had smaller effects at 7 kHz. The notable exception to these trends is the 1.0 mm thick graft with bone contact condition at 4 kHz, which showed a 6 dB decrease in impedance magnitude averaged over the 3 bones. Much of this decrease comes from bone 10, where the placement of the cartilage in that condition produced a significant increase in TM motion.

DISCUSSION

Cartilage is commonly placed in the posterior-superior quadrant of the TM to cover ossicular prostheses and minimize their extrusion (Yung, 2008; Tos, 2008). We studied the effects of cartilage placements in the posterior and posterior-superior part of the TM, with and without bony support, on sound-induced TM motion with stroboscopic holography.

We have previously reported time-averaged holography and laser-Doppler vibrometry results relevant to this question. Time-averaged holograms describe the spatial patterns of the sound-induced motion of the surface of the TM of cadaveric temporal bones to tones of varied frequencies and levels (Aarnisalo et al., 2009). Our data suggested that the thickness and positioning of the cartilage plates has little adverse effect on the mechanics of the tympanoplasty, keeping in mind that our study was restricted to cartilage plates that were 6 × 3 mm in size and 0.5 or 1.0 mm thick.

The displacement amplitude of the whole TM was evaluated with the stroboscopic holography technique. The site of maximum displacement was not changed at low frequencies with different TM conditions (0.5 and 1 kHz). At high frequency measurements (4 kHz, 7–8 kHz), a local area with no motion or reduced motion could be seen. Other areas of the TM showed similar or even increased motion compared to the control condition. These displacement amplitude maps are in agreement with our time-averaged data with TM motion (Aarnisalo et al., 2009).

Measurements of the TM displacement amplitude along a 45° degree diameter in the different conditions showed that cartilage plates on the posterior-superior part of TM, with both thicknesses and positions, decreased the TM motion at 0.5 and 1 kHz in all three bones studied, which was not readily seen in our time-averaged holograph measurements (Aarnisalo et al. 2009). At higher frequencies the cartilage also caused a significant reduction in motion of the area of the TM apposed to the graft, except with temporal bone TB 10 with the 1.0 mm thick graft, consistent with our time-averaged hologram findings. We conclude, the stroboscopic mode measurement not only allows quantification of magnitude and phase of motion, but is also a more sensitive method to study changes in TM displacement.

Our earlier studies with laser-Doppler vibrometry (with these same bones) show only minor cartilage-induced changes in the stapes velocity with frequencies of 0.5 and 1 kHz (8 dB or less) and 4 kHz-8 kHz (4 dB or less) (Aarnisalo et al., 2009). While the reductions in TM motion magnitude at 0.5 and 1 kHz are comparable to the 8 dB alterations in stapes velocity at the these frequencies, the combination of large cartilage-induced alterations in the TM displacement magnitudes at 4 and 8 kHz and no measurable effects on stapes velocity is consistent with the hypothesis that large regions of the TM are uncoupled from the ossicular chain with high-frequency sound stimulation (Tonndorf and Khanna, 1970;1971; Shaw and Stinson, 1983).

Our estimates of middle-ear input impedance, based on the summation of velocities on the TM surface, are similar to the acoustic measurements of Rabinowitz (1981) and others at 1 kHz, but are somewhat larger at 0.5 kHz and 4 kHz (the upper limit of Rabinowitz's measurements). A complication in comparing our impedance estimates at 4, 7 and 8 kHz with existing measurements is that it is difficult to directly measure the acoustic input impedance at the TM at these high frequencies, and most of our knowledge of human TM acoustics above 2 kHz comes from acoustic reflectance estimates made more peripherally in the ear canal (Stinson et al., 1982; Hudde, 1983; Keefe et al. 1993; Voss and Allen, 1994). The significant increase in impedance magnitude we estimate at 4, 7 and 8 kHz is consistent with the increased reflectance observed by most of these studies at those frequencies.

The cartilage generally produced increases in middle ear impedance especially at 1 kHz with the 1.0 mm thick cartilage graft that was not in contact with bone, and 4 kHz with both 0.5mm and 1.0 mm thick grafts without bony contact. At 4 kHz, the 1.0 mm thick graft with bony contact produced decrease in the mean impedance compared to the controls. The impedance is consistent with the spatial magnitude maps of these three bones. The occasional decreases in the impedance that we observed can be explained with increased motion of other areas of the TM that are not covered by the cartilage graft.

Single-point laser-interferometry velocity measurements near the umbo have been used to investigate the effect of various TM and ossicular pathologies on middle ear function (Voss et al., 2001; Goode et al., 1993; Rosowski et al., 2008). Conductive pathologies that reduce umbo velocity also reduce stapes velocity. However, the reductions of stapes and umbo velocity need not to be proportional (Nakajima et al., 2005; Rosowski et al., 2008). Pathologies that interrupt the continuity of the ossicular chain lead to increased TM and umbo velocities while the stapes velocity is greatly reduced (Rosowski et al., 2008). The relationship between the vibration of the reconstructed TM and stapes velocity is complicated due to the complex structure and geometry of the TM. Local displacement changes, even when the cartilage is placed at the area of displacement maxima, seem to have little effect on the stapes velocity.

Murbe et al. (2002) suggested that if a cartilage graft is suspended from the osseous annular rim, the acoustic transfer characteristics of the reconstructed TM are determined by stiffness of the cartilage. A cartilage island with a regular TM surrounding it influences the vibrational characteristics mainly by mass of the cartilage, as the stiffness of the membrane is determined by the surrounding TM remnant. With the stroboscopic holography technique, we saw only small differences in the maximum motion of the TM at 500 Hz and 1 kHz, or in the velocity of the stapes at any frequency when our cartilage plates were positioned so that they were either in contact with the bony tympanic rim and manubrium or not.

Murbe et al. (2002) suggested that small cartilage transplants, embedded in a normally vibrating TM, will influence the vibration pattern of the TM only at a small frequency band, if the cartilage lies in a region of the maximum displacement of membrane. Our stroboscopic holography results with 0.5 mm and 1.0 mm thick grafts showed decreases in the maximum displacement of the TM at low frequencies (500 Hz and 1 kHz) and changes in the motion pattern 4 kHz and above. Only minor changes in stapes velocity were observed at any frequency studied (Aarnisalo et al., 2009).

In summary, we found alterations in the pattern of TM displacement after cartilage placement on the medial side of TM at all the studied frequencies, but those changes seemed not to be associated with changes in stapes velocity. Our results indicate that small cartilage grafts in the posterior-superior TM quadrant can protect the TM from prosthetic extrusion or graft retraction and not greatly affect middle-ear function irrespective of the thickness of the cartilage and its contact with the bony tympanic rim and manubrium, at least for frequencies below 7–8 kHz.

Conclusions

Middle ear mechanics can be studied with stroboscopic holography after tympanoplasty. Covering the posterior-superior quadrant of the TM with thick or thin cartilage produce significant local changes in TM motion but have little effect on middle-ear sound transmission below 7–8 kHz. Also, allowing the cartilage to extend a little beyond the bony annulus to help prevent postoperative TM retraction does not adversely affect middle ear sound transmission.

Acknowledgments

We would like to thank the staff at Eaton-Peabody laboratory. This study was supported by the National Institute on Deafness and Other Communication Disorders, Mr Lakshmi Mittal, Mr. Axel Eliasen and the Academy of Finland.

References

Aarnisalo AA, Cheng JT, Ravicz ME, Hulli N, Harrington EJ, Hernandez-Montes MS, Furlong C, Merchant SN, Rosowski JJ. Middle Ear Mechanics of Cartilage Tympanoplasty Evaluated by Laser Holography and Vibrometry. Otology Neurotology. 2009 epub ahead of print.

Cheng JT, Aarnisalo AA, Merchant SN, Furlong C, Rosowski JJ. The motion of the surface of the human tympanic membrane measured with stroboscopic holography. 2009 Submitted, Hearing Research.

Chien W, Ravicz ME, Merchant SN, Rosowski JJ. The effects of methodological differences in the measurement of stapes motion in live and cadaver ears. Audiol Neurootol 2006;11(3):183–97. [PubMed: 16514236]

Decraemer WF, Khanna SM, Funnell WRJ. Vibration at a fine grid of points on the cat tympanic membrane measured with a heterodyne interferometer. EOS/SPIE Int Sym, Munchen. 1999

de La Rochefoucauld O, Olson E. A sum of simple and complex motions on the eardrum and manubrium in gerbil. 2009 Submitted, Hearing Research.

Furlong C, Pryputniewicz RS. Hybrid computational and experimental approach for the study and optimization of mechanical components. Opt Eng 1998;37(5):1448–55.

Furlong C, Rosowski JJ, Hulli N, Ravicz ME. Preliminary analyses of tympanic-membrane motion from holographic measurements. Strain. 2009 In-press. 10.1111/j.1475–1305.2008. 00490.x.

Goode RL, Ball G, Nishihara S. Measurement of umbo vibration in human subjects - methods and possible clinical applications. Am J Otol 1993;14:247–251. [PubMed: 8372921]

Hernández-Montes MDS, Furlong C, Rosowski JJ, Hulli N, Harrington E, Cheng JT, Ravicz ME, Santoyo FM. Optoelectronic holographic otoscope for measurement of nano-displacements in tympanic membrane. J Biomed Optics. 2009 In press.

Hudde H. Measurement of the eardrum impedance of human ears. J Acoust Soc Am 1983;73:242–247. [PubMed: 6826891]

Keefe DH, Bulen JC, Arehart KH, Burns EM. Ear-canal impedance and reflection coefficient in human infants and adults. J Acoust Soc Am 1993;94:2617–2638. [PubMed: 8270739]

Lee CF, Hsu LP, Chen PR, Chou YF, Chen JH, Liu TC. Biomechanical modeling and design optimization of cartilage myringoplasty using finite element analysis. Audiol Neurootol 2006;11(6):380–8. [PubMed: 16988502]

Lee CF, Chen JH, Chou YF, Hsu LP, Chen PR, Liu TC. Optimal graft thickness for different sizes of tympanic membrane perforation in cartilage myringoplasty: A finite element analysis. Laryngoscope 2007;117(4):725–730. [PubMed: 17415145]

Murbe D, Zahnert T, Bornitz M, Huttenbrink KB. Acoustic properties of different cartilage reconstruction techniques of the tympanic membrane. Laryngoscope 2002;112:1769–76. [PubMed: 12368613]

Nakajima HH, Ravicz ME, Merchant SN, Peake WT, Rosowski JJ. Experimental ossicular fixations and the middle ear's response to sound: evidence for a flexible ossicular chain. Hear Res 2005;204(1–2):60–77. [PubMed: 15925192]

Rabinowitz W. Measurement of the acoustic input immittance of the human ear. J Acoust Soc Am 1981;70:1025–1035. [PubMed: 7288039]

Rosowski JJ, Nakajima HH, Merchant SN. Clinical utility of laser-Doppler vibrometer measurements in live normal and pathologic human ears. Ear Hear 2008;29(1):3–19. [PubMed: 18091103]

Rosowski JJ, Cheng JT, Ravicz ME, Hulli N, Hernandez-Montes M, Harrington E, Furlong Cosme. Computer-assisted time-averaged holography of the motion of the surface of the tympanic membrane with sound stimuli of 0.4 to 25 kHz. Hear Res. 2009 In press. 10. 1016/j.heares.2009.03.010

Schuknecht H. Temporal bone removal at autopsy. Preparation and uses Arch Otolaryngol 1968;87:129–137.

Shaw, EG.; Stinson, MR. The human external and middle ear: Models and concepts. In: deBoer, E.; Viergever, MA., editors. Mechanics of Hearing. Delft University Press; 1983. p. 3-10.

Stinson MR, Shaw EAG, Lawton BW. Estimation of acoustical energy reflectance at the eardrum from measurements of pressure distribution in the ear canal. J Acoust Soc Am 1982;72:766–773. [PubMed: 7130535]

Tonndorf J, Khanna SM. The role of the tympanic membrane in middle ear transmission. Ann Otol 1970;79:743–753.

Tonndorf J, Khanna SM. The tympanic membrane as a part of the middle ear transformer. Acta Otolaryngol 1971;71:177–80. [PubMed: 5577012]

Tos M. Cartilage tympanoplasty methods: proposal of a classification. Otolaryngol Head Neck Surg 2008;139(6):747–58. [PubMed: 19041498]

Voss SE, Allen JB. Measurement of acoustic impedance and reflectance in the human ear canal. J Acoust Soc Am 1994;95:372–384. [PubMed: 8120248]

Voss SE, Rosowski JJ, Merchant SN, Peake WT. How do tympanic-membrane perforations affect human middle-ear sound transmission? Acta Otolaryngol 2001;121:169–173. [PubMed: 11349771]

Wada H, Ando M, Takeuchi M, Sugawara H, Koike T. Vibration measurement of the tympanic membrane of guinea pig temporal bones using time averaged speckle pattern interferometry. J Acoust Soc Am 2002;111(5):2189–99. [PubMed: 12051438]

Yung M. Cartilage tympanoplasty: literature review. J Laryngol Otol 2008;122:663–72. [PubMed: 18312709]

Zahnert T, Huttenbrink KB, Murbe D, Bornitz M. Experimental investigations of the use of cartilage in tympanic membrane reconstruction. Am J Otol 2000;21(3):322–8. [PubMed: 10821543]

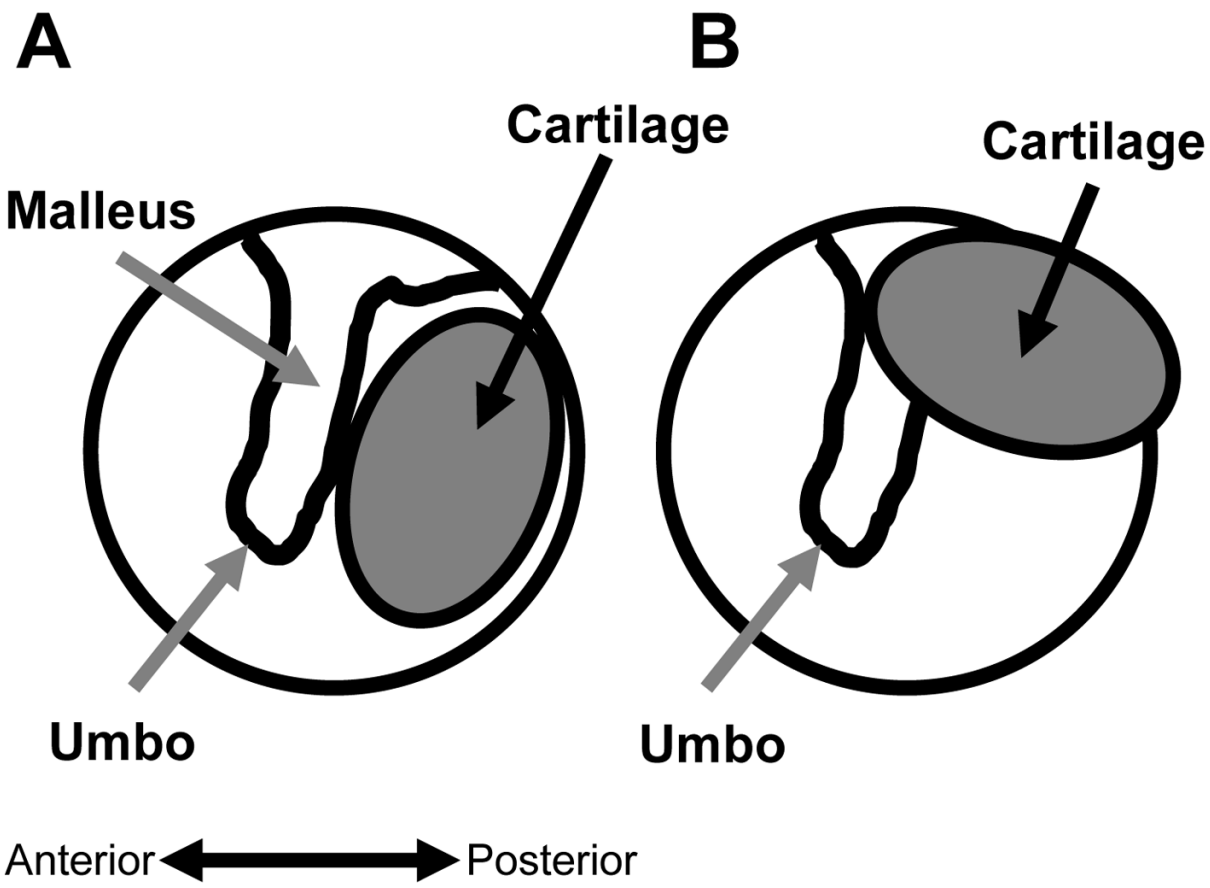

Figure 1.
A schematic drawing showing the position of the oval shaped, 6mm × 3mm sized cartilage graft. In A) the graft is not in contact with the bony tympanic rim and manubrium. In B) the graft is rotated so that it is in contact with the bony tympanic rim and manubrium. Arrows are showing the cartilage graft, malleus and umbo.

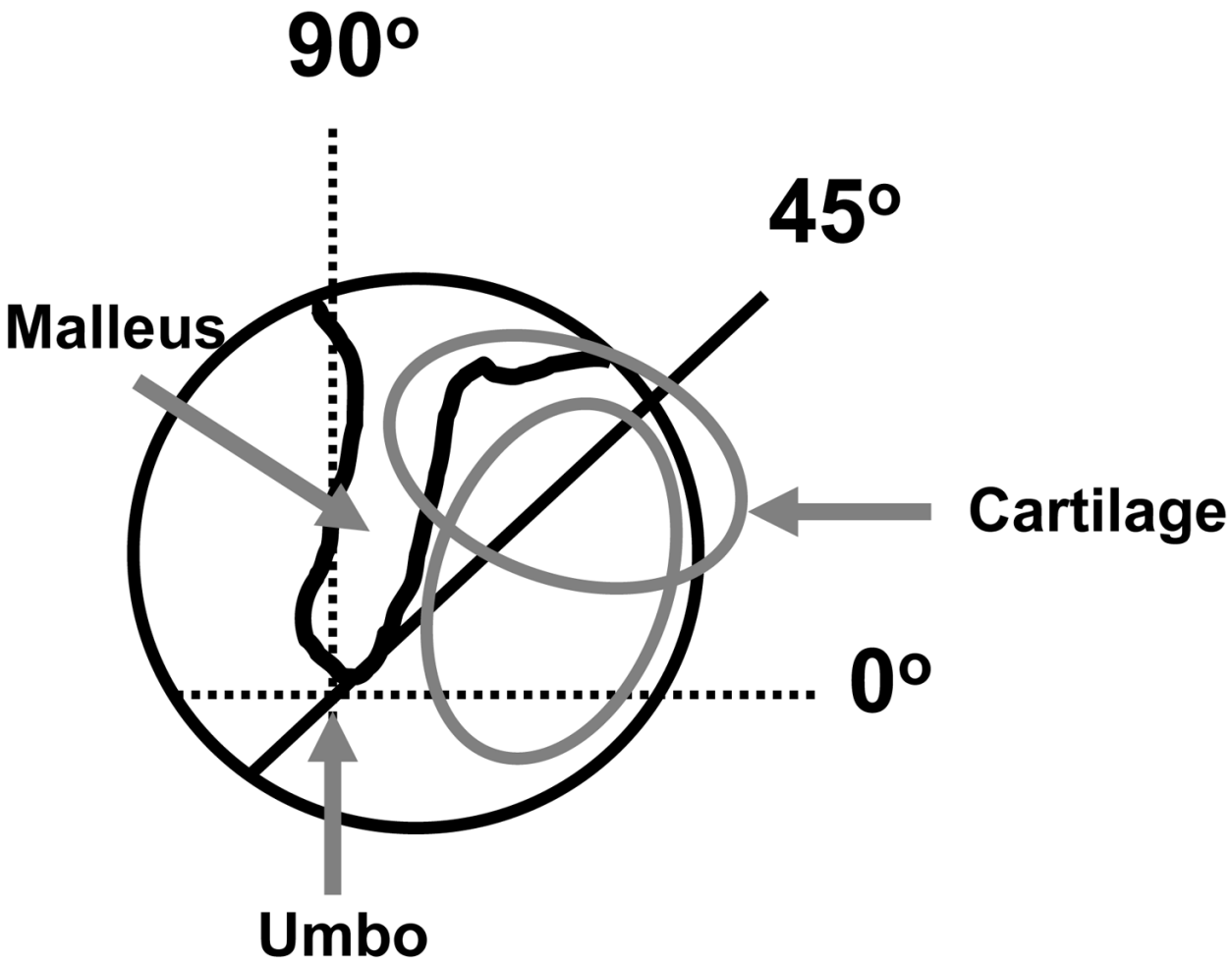

Figure 2.
A schematic drawing showing the entire TM with individual chords (0°, 45°, 90°). The crossing point of these chords is at the umbo. The gray ovals show the two different positions of the cartilage graft. The 45° chord crosses the area covered by the grafts.

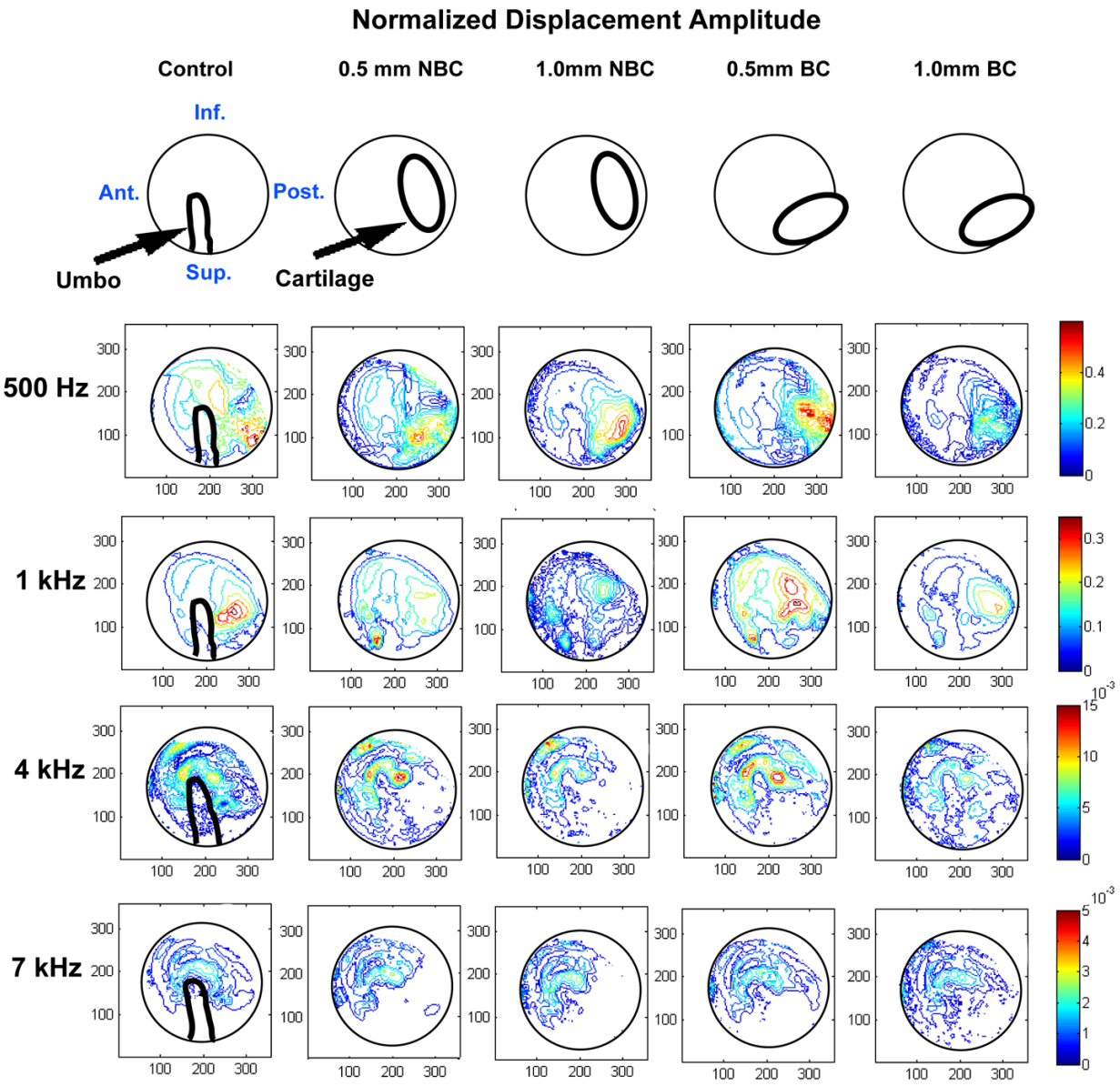

Figure 3.

Displacement amplitude of the whole TM.

The magnitude of motion can be seen with different conditions. The data is normalized by the pressure. The position of the cartilage can be seen in the upper row. Cartilage that is positioned so that it is in contact with the bony tympanic rim produces smaller areas with little motion compared to the situation when the cartilage graft has no bony contact. For orientation the posterior (Post.), anterior (Ant.), superior (Sup.) and inferior (Inf.) are shown. Umbo, malleus and the cartilage sheet position are indicated in the schematics in the top row. The maps code displacement amplitude from zero (deep blue) to maximum (dark red). 0.5mm/1.0mm NBC/BC = 0.5mm/1.0mm no bony contact/with bony contact.

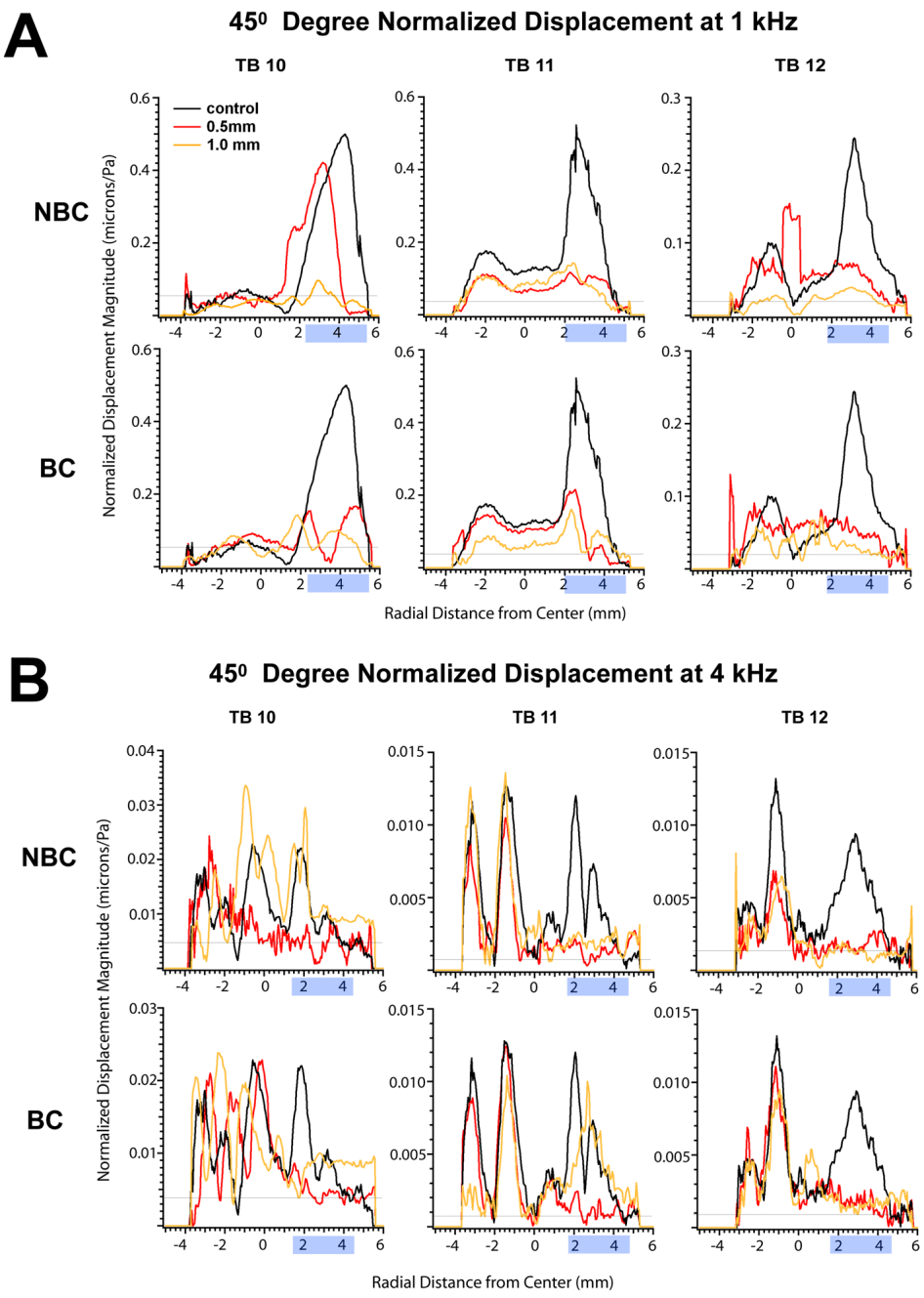

Figure 4.

Displacement Amplitude along the 45° chordal diameter on the TM Surface. Both at 1 kHz and 4 kHz frequencies, along the 45° diameter on the TM surface, a reduction can be seen in the motion of TM in the region covered by the cartilage plate, except with the 1.0 mm thick graft in TB10. The umbo is at the 0 mm position. The blue shading in the x axis label shows the position of the cartilage graft.

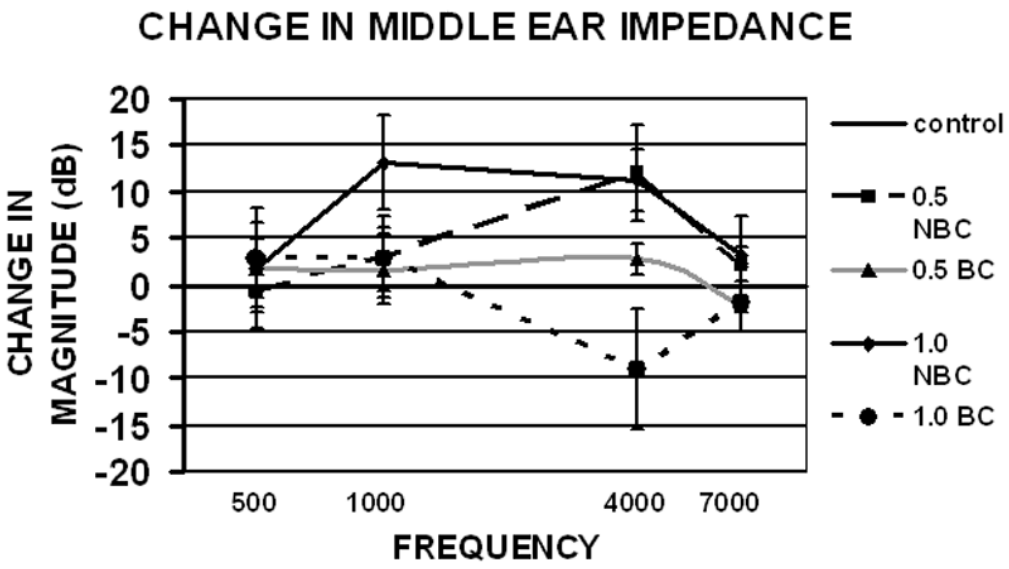

Figure 5.

The change in the middle ear impedance. Results of three bones are averaged (± S.D.). 0.5mm/1.0mm NBC/BC = 0.5mm/1.0mm thick graft with no bony contact/with contact to the tympanic rim and manubrium.

Table 1

The impedance magnitude calculated in the normal condition in our three temporal bones at four frequencies. The data of Rabinowitz (1981) is included for comparison.

Input Impedance at the Tympanic Membrane (mks MOhm)				
Frequency	**TB10**	**TB11**	**TB12**	**Rabinowitz 1981**
0.5 kHz	130	150	104	60
1. kHz	36	36	54	40
4 kHz	160	320	180	38
7 kHz	—	800	720	—
8 kHz	380	—	—	—